Delayed Cracking in a Metastable Austenitic Stainless Steel

Petr Haušild[1,a], Philippe Pilvin[2,b] and Michal Landa[3,c]

[1] Department of Materials, Faculty of Nuclear Sciences and Physical Engineering, Czech Technical University, Trojanova 13, 120 00 Praha 2, Czech Republic

[2] Laboratoire d'Ingénierie des Matériaux de Bretagne, Université de Bretagne-Sud, Rue de Saint-Maudé, BP 92116, 56321 Lorient, France

[3] Institute of Thermomechanics, Academy of Sciences of the Czech Republic, Dolejškova 5, 182 00 Praha 8, Czech Republic

[a]petr.hausild@fjfi.cvut.cz, [b]philippe.pilvin@univ-ubs.fr, [c]ml@it.cas.cz

Keywords: Delayed cracking; Martensitic transformation, Acoustic emission; Fractography

Abstract. The mechanical properties of metastable austenitic steel were characterized by means of tensile testing and cupping tests. High sensitivity to the strain rate was observed. The fracture mechanism in tensile specimens at the strain rate lower than $\dot{\varepsilon}=10^{-3}$ s^{-1} was the combination of cleavage and ductile dimpled rupture. At the strain rate higher than $\dot{\varepsilon}=10^{-3}$ s^{-1} fracture mechanism changed to entire ductile dimpled rupture. Fracture mechanisms were very different in tensile specimens and in deep drawn cups. After deep drawing tests with drawing ratios DR > 1.5 delayed cracking occurred. Main fractographic feature observed in cracked deep drawn cups was the intergranular decohesion.

Introduction

Austenitic stainless steels have an excellent corrosion resistance, good mechanical properties and are widely used for cold forming (deep-drawing) at room temperature. Increasing need for conserving the strategic elements such as nickel and chromium impel the steel-makers to lower the content of these elements in stainless steels. However, the low nickel content can lead during the forming process to the plastic deformation-induced phase transformation of face-centered cubic (fcc) γ austenite to body-centered cubic (bcc) α' martensite [1-4]. High internal stresses are generated due to an incompatible transformation strain accompanying the martensitic transformation (shear strain of 20% can cause a volume change of 2% [5]). The residual stresses together with the internal stresses induced by martensitic transformation can lead after deep-drawing to the phenomenon of delayed cracking. The good knowledge of kinetics of the martensitic transformation is therefore an essential constituent for a control of the forming process.

The evolution of martensitic volume fraction is monitored by acoustic emission (AE) and Electron Back-Sacttering Diffraction (EBSD). The AE technique provides a method to detect rapid micromechanical events, such as avalanche dislocation movement, mechanical twinning, or microcracking [6,7]. AE technique was successfully used for monitoring of strain induced martensitic transformation in Fe-Ni-C alloy [8]. Combining this method with metallographic and fractographic analyses, different stages of physical processes in material such as phase transformation or damage can be identified.

Experimental Details

The material chosen for this study was austenitic steel corresponding to the AISI301. The chemical composition is given in Table 1. The low nickel and chromium content situates the steel at the limit of the austenite field in the phase diagram. The material was provided by the ARCELOR as cold rolled sheets of 0.68 mm thickness in the bright annealed state.

Table 1 Chemical composition of AISI301 steel (in wt.%).

	C	*Cr*	*Ni*	*Si*	*Mn*	*Mo*
nominal	Max 0.12	16-18	6,5-9	<1,5	<2	<0,8
	0,05	17	7	0,5	1,5	0,1

The tensile tests were carried out on an INSPEKT 100kN testing machine at room temperature imposing various strain rates ranging from $\dot{\varepsilon}=5.10^{-5}$ s^{-1} to $\dot{\varepsilon}=5.10^{-2}$ s^{-1}. Temperature increase during tests was measured by a thermocouple.

The AE signal was monitored during selected tensile test using a highly sensitive transducer coupled to the specimen head. A computer controlled DAKEL-XEDO-6 AE facility was used to record the AE counts. The AE facility applied a two threshold level system of detection and evaluation of AE, recently recommended by an ASTM standard. The lower threshold level was 556 mV, the higher threshold level was 1200 mV. The total gain was about 100 dB.

Cup drawing tests were carried out on a 500kN INSTRON testing machine using punch diameter 100 mm and different drawing ratios.

Microstructure was revealed by electro-polishing in 5% perchloric acid solution in ethanol at 40V and etching in 1:1:1 solution of H_2O, HCl and HNO_3. Fractured tensile specimens and cracked cups were carefully examined in the Scanning Electron Microscope (SEM) JSM 5510LV. The martensite volume fraction was characterized by EBSD in SEM FEI Quanta 200 FEG equipped with a TSL™ EBSD analyzer. Acquired data were evaluated by OIM™ software.

Results

Tensile test. Results of tensile tests at room temperature with strain rates ranging from $\dot{\varepsilon}=5.10^{-5}$ s^{-1} to $\dot{\varepsilon}=5.10^{-2}$ s^{-1} are shown in Fig.1. One can see in Fig. 1 the change in the slope of stress-strain curves (increase of the hardening rate) due to the presence of martensitic phase. The shape of stress-strain curves is strongly dependent on strain rate. With increasing strain rate yield stress increases, ultimate tensile strength decreases and elongation to fracture has a maximum at $\dot{\varepsilon}=5.10^{-3}$ s^{-1}.

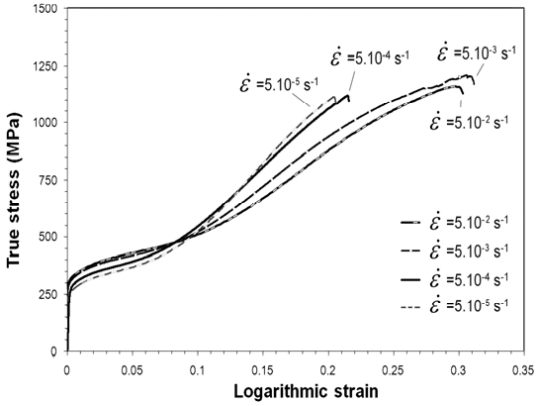

Fig. 1 Stress-strain curves of AISI301 steel tested at room temperature at different strain rates.

During the tensile tests at higher strain rates ($\dot{\varepsilon}=5.10^{-3}$ s^{-1} and $\dot{\varepsilon}=5.10^{-2}$ s^{-1}), the heating of specimens occurred (Fig. 2). The measured temperature increase ΔT was nearly the same as obtained by integrating the formula:

$$dT = \frac{1}{\rho C_p}\left(0.9\sigma_{eq}\, d\varepsilon_{eq}^{pl} + \Delta H_m df_m - \lambda \frac{dT}{dx} dt\right) \quad (1)$$

Where ρ is the density (8000kg.m^{-3}), C_p the thermal capacity (500J.kg^{-1}.K^{-1}), H_m the enthalpy of martensitic transformation (10000J.kg^{-1}), f_m the martensitic volume fraction and λ the thermal conductivity of steel (16.2W.m^{-1}.K^{-1}). First term in brackets corresponds to the 90% of plastic deformation energy converted to the heating, second term to the transformation heat and third term to the heat removal by thermal conduction (to jaws only).

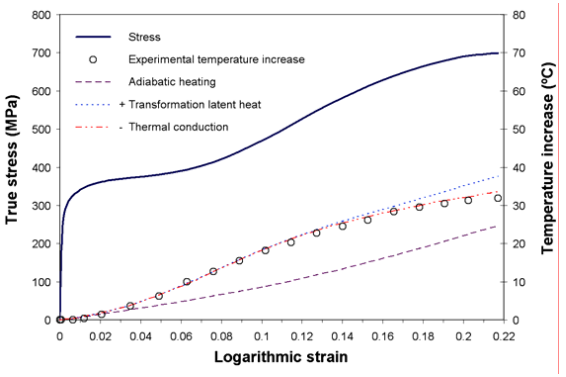

Fig. 2 Heating of specimen during the tensile test of AISI301 steel tested at $\dot{\varepsilon}$=5.10^{-3} s^{-1}.

Acoustic emission. A typical AE captured during the tensile test is shown in Fig. 3. There is a well defined AE response throughout the total loading time. Several AE pulses are observed after the yielding. First, there is an increase in the AE activity. Before reaching the level of deformation corresponding to the change of hardening rate, AE activity slightly decreased, as can be seen in the decreasing slope of the AE count. The typical S-shape of AE count curve is also illustrated in the Fig. 4. In the case of the test at the strain rate $\dot{\varepsilon}$=5.10^{-4} s^{-1}, the final fracture was preceded by several distinct high energy acoustic events. The rise time of these events was about three times higher than the rise time of the previous events corresponding to the martensitic transformation. No such events were observed during the tests at the strain rates $\dot{\varepsilon}$=5.10^{-3} s^{-1} and $\dot{\varepsilon}$=5.10^{-2} s^{-1}.

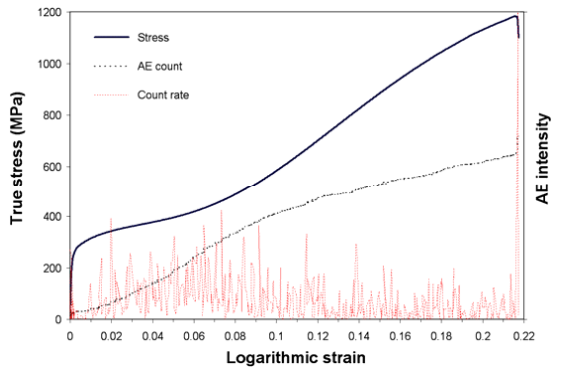

Fig. 3 AE during the tensile test of AISI301 steel tested at room temperature at $\dot{\varepsilon}$=5.10^{-4} s^{-1}.

Microstructure. For the observing the changes in microstructure caused by martensitic transformation, four specimens were tensile pre-deformed to 5, 10, 15 and 20 % of (logarithmic) plastic deformation and compared with non-deformed state. Strain rate for pre-deformation was chosen $\dot{\varepsilon}=5.10^{-4}$ s^{-1} in order to avoid the heating of specimens. In Fig. 4 is shown the microstructure in non-deformed state (as-received) and after 2.5%, 5%, 10%, 15% and 20 % of plastic deformation. In non-deformed state, the microstructure is composed of equiaxed austenitic grains with typical annealing twins. After 2.5% of plastic deformation, several martensitic variants can be seen inside the austenitic grains. After 15 % of plastic deformation, the microstructure is mostly martensitic.

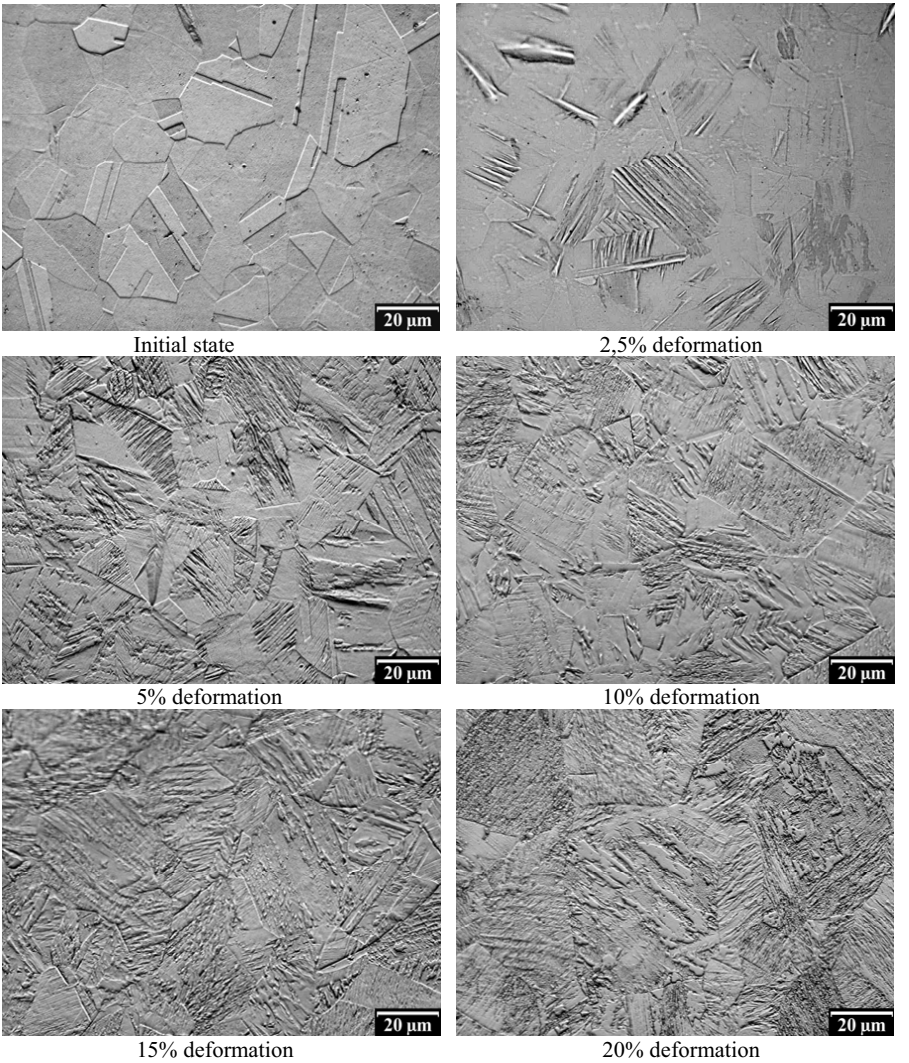

Fig. 4 Microstructure of AISI301 steel (light microscopy) in non-deformed state and after different tensile pre-deformation.

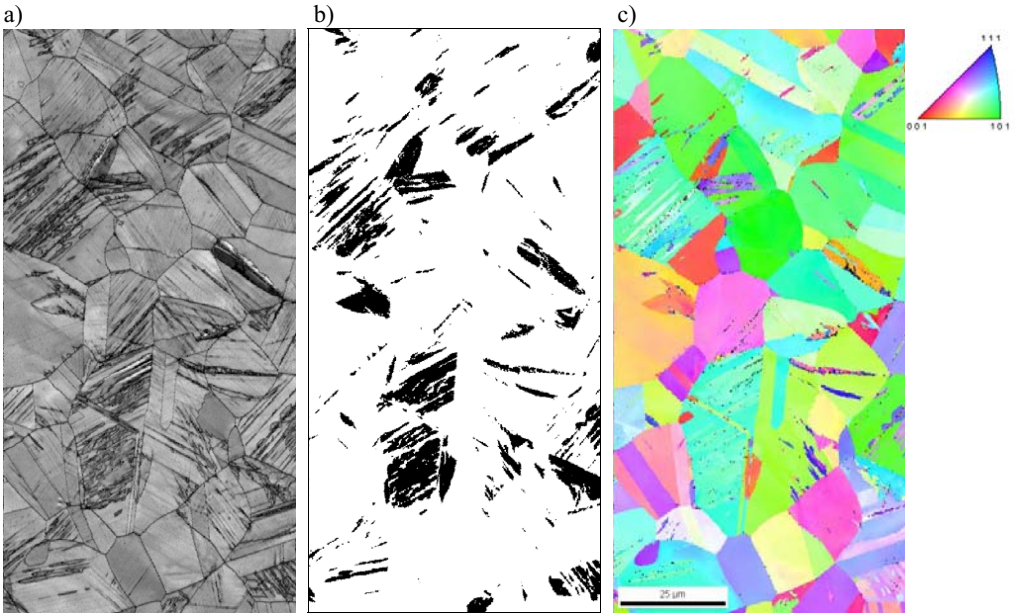

Fig. 5 Apparition of martensite in AISI301 steel after 5% of tensile pre-deformation (EBSD). Image quality (a), phase content (b), inverse pole figures (c).

Fractography. Fracture surfaces of tensile specimens tested at the strain rates $\dot{\varepsilon}=5.10^{-5}$ s^{-1} and $\dot{\varepsilon}=5.10^{-4}$ s^{-1}, were oriented in perpendicular to the loading axis whereas the fracture surfaces of tensile specimens tested at the strain rates $\dot{\varepsilon}=5.10^{-3}$ s^{-1} and $\dot{\varepsilon}=5.10^{-2}$ s^{-1}, were inclined of about 45º. Fractographic analysis of specimens broken at the strain rate $\dot{\varepsilon}=5.10^{-5}$ s^{-1} and $\dot{\varepsilon}=5.10^{-4}$ s^{-1} revealed several transgranular cleavage facets connected by ductile dimpled rupture (Fig. 6). Several slip bands can be found on cleavage facets which indicate that the cleavage facets were formed before the final ductile fracture. On the other hand, the fracture surfaces of tensile specimens tested at the strain rates $\dot{\varepsilon}=5.10^{-3}$ s^{-1} and $\dot{\varepsilon}=5.10^{-2}$ s^{-1}, are completely covered by ductile dimples (Fig. 7).

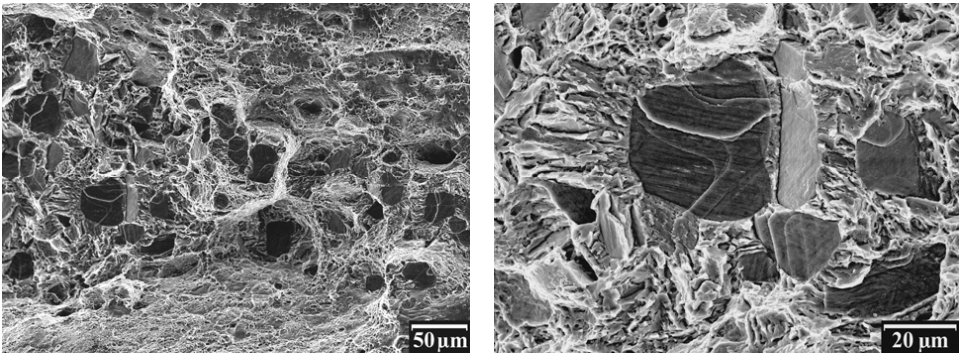

Fig. 6 Fracture surfaces of tensile specimens tested at room temperature at $\dot{\varepsilon}=5.10^{-4}$ s^{-1}.

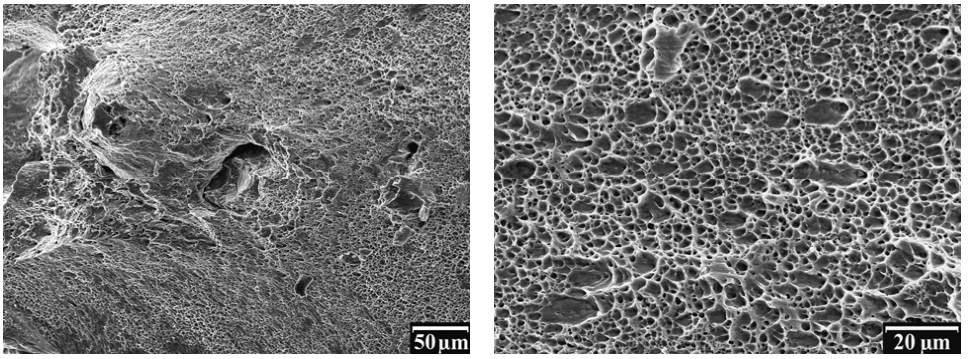

Fig. 7 Fracture surfaces of tensile specimens tested at room temperature at $\dot{\varepsilon}=5.10^{-3}$ s^{-1}.

Fig. 8 Delayed cracking after deep drawing test in cups with different drawing ratios.

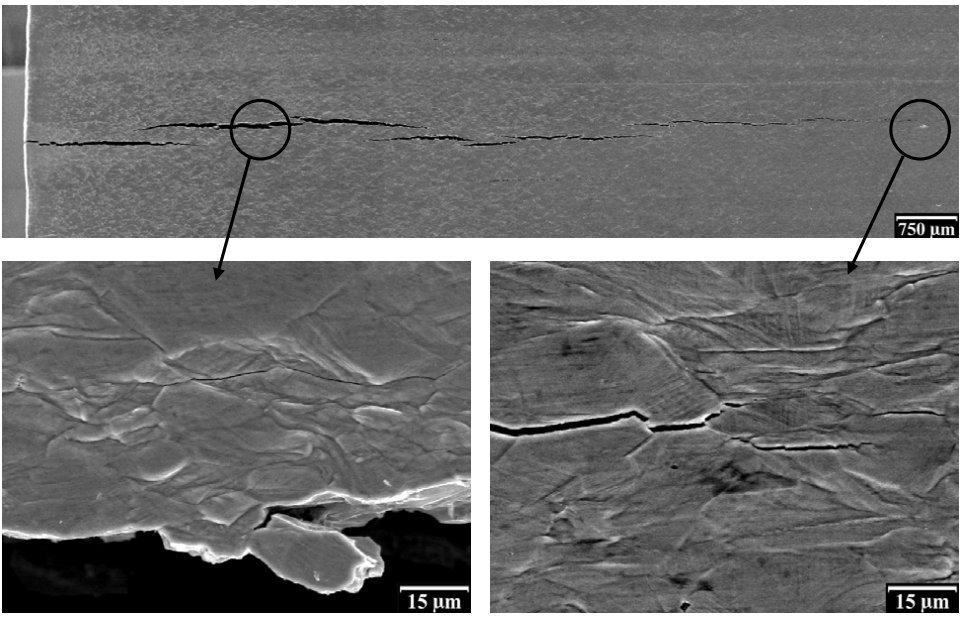

Fig. 9 Crack propagation on the lateral face of the cup.

Delayed cracking. Delayed fracture occurred in the cups (Fig.8) after deep drawing tests with drawing ratios DR > 1.5. On the lateral face several more or less equidistant arrested cracks can be observed. Cracks arrested in the cup wall at about the same height as the height of cup with initial drawing ratio DR ~ 1.4.

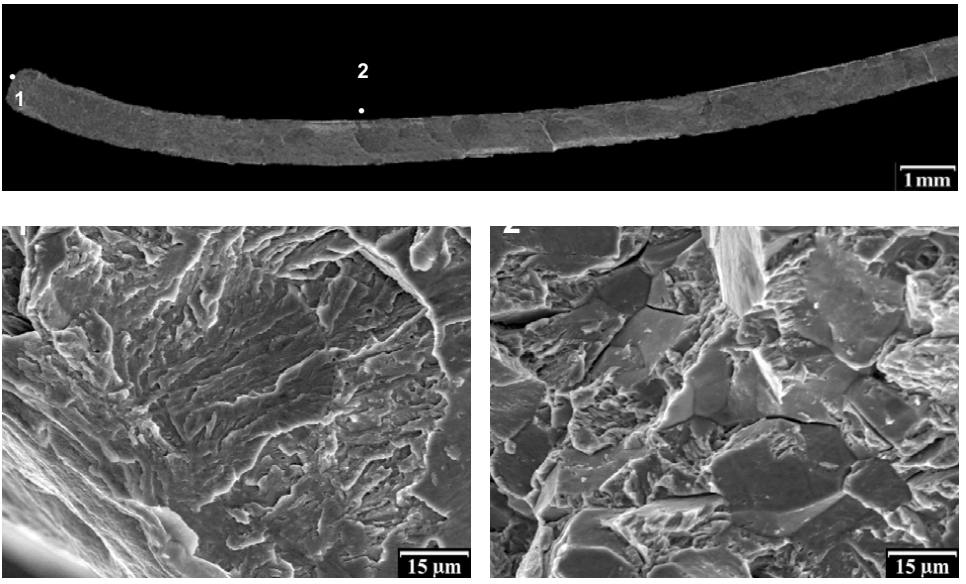

Fig. 10 Fracture surface of the cup cracked after deep drawing test - transgranular crack initiation on the top of the cup (1) and intergranular decohesion in the center of the cup's wall (2).

Lateral faces and cracks in the cups issued from deep drawing tests were analyzed in SEM (Fig.9). Cracks propagated by the mechanism of diffused damage - several microcracks were found in proximity of principal crack lips and ahead of the crack tips. Micromechanism of crack propagation was as well transgranular as intergranular.

On the fracture surfaces of opened cracks, several fractographic features were found: cleavage facets, intergranular decohesion and ductile tearing. Crack initiated on the top of the cup (probably on the surface technological defect) by the mechanisms of transgranular cleavage or quasi-cleavage (Fig.10). In the center of the cup's wall, the main feature observed was the intergranular decohesion.

Summary

The results of the study presented can be summarized as follows:

- Mechanical response of AISI301 steel is very sensitive to the strain rate due to the coupling of thermo-mechanical behaviors. Fracture mechanism in tensile specimens at the strain rate lower than $\dot{\varepsilon}=10^{-3}$ s^{-1} is the combination of cleavage and ductile dimpled rupture. At the strain rate higher than $\dot{\varepsilon}=10^{-3}$ s^{-1} fracture mechanism changes to entire ductile dimpled rupture.
- Monitoring of acoustic emission during the tensile test revealed several features. AE is generated by a sudden local rearrangement of the internal stress field and can therefore be produced only by rapid events such as twinning or microcracking. AE pulses occur in the loading history at the same time as developing plastic deformation causes the martensitic transformation. The pulses were probably generated by twinning or slip accompanying the shear (displacive)

transformation.

- Delayed cracking occurred after cupping tests. Fracture mechanisms are very different in tensile specimens and deep drawn cups. Main fractographic feature observed in cracked deep drawn cups was the intergranular decohesion.

Experimental data presented in this paper provide a useful guide for the development of numerical models for simulation of deformation behaviors and phase transformation of metastable austenitic steels subjected to large deformation.

Acknowledgement

Authors wish to thank the Arcelor-Mittal group for supplying the material. This work was supported by the Ministry of Education, Youth and Sports of the Czech Republic in the frame of the research project MSM 6840770021.

References

[1] L. Mangonon Jr., G. Thomas, Met. Trans. 1 (1970) 1577–1586.

[2] T. Suzuki, H. Kojima, K. Suzuki, T. Hashimoto, M. Ichihara, Acta Met. 25 (1977) 1151–1162.

[3] J.W. Brooks, M.H. Loretto, R.E. Smallman, Acta Met. 27 (1979) 1839–1847.

[4] M. Humbert, B. Petit, B. Bolle, N. Gey, Mater. Sci. Eng. A 454–455 (2007) 508–517.

[5] I. Timokhina, P. Hodgson, E. Pereloma, Effect of alloying elements on the microstructure-property relationship in thermomechanically processed C-Mn-Si TRIP steels, in: B.C. De Cooman (Ed.), Proceedings of the International Conference on TRIP-aided High Strength Ferrous Alloys, Ghent, 2002, pp. 153-157.

[6] C.R. Heiple, S.H. Carpenter, J. Acoust. Emiss. 6 (1987) 177 – 204.

[7] C.R. Heiple, S.H. Carpenter, J. Acoust. Emiss. 6 (1987) 215 – 237.

[8] Q.Y. Long, Z. Zhu, X.M. Zhang, D.F. Li, Scripta Metall. Mater. 26 (1992) 1095-1100.